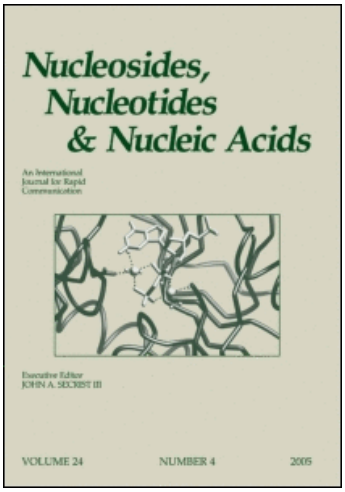

Nucleosides, Nucleotides and Nucleic Acids
Publication details, including instructions for authors and subscription information:
http://www.informaworld.com/smpp/title~content=t713597286

A COMPARISON OF THE PROPERTIES AND THE SOLUTION STRUCTURE FOR RNA AND DNA QUADRUPLEXES WHICH CONTAIN TWO GGAGG SEQUENCES JOINED WITH A TETRANUCLEOTIDE LINKER

Hui Liu[a]; Atsushi Kugimiya[a]; Tokuhiro Sakurai; Masato Katahira[a]; Seiichi Uesugi
[a] Department of Environment and Natural Sciences, Graduate School of Environment and Information Sciences, Yokohama National University, Yokohama, Hodogaya-ku, Japan

Online publication date: 12 February 2002

To cite this Article Liu, Hui , Kugimiya, Atsushi , Sakurai, Tokuhiro , Katahira, Masato and Uesugi, Seiichi(2002) 'A COMPARISON OF THE PROPERTIES AND THE SOLUTION STRUCTURE FOR RNA AND DNA QUADRUPLEXES WHICH CONTAIN TWO GGAGG SEQUENCES JOINED WITH A TETRANUCLEOTIDE LINKER', Nucleosides, Nucleotides and Nucleic Acids, 21: 11, 785 — 801
To link to this Article: DOI: 10.1081/NCN-120016481
URL: http://dx.doi.org/10.1081/NCN-120016481

MARCEL DEKKER, INC. • 270 MADISON AVENUE • NEW YORK, NY 10016

NUCLEOSIDES, NUCLEOTIDES & NUCLEIC ACIDS
Vol. 21, Nos. 11 & 12, pp. 785–801, 2002

A COMPARISON OF THE PROPERTIES AND THE SOLUTION STRUCTURE FOR RNA AND DNA QUADRUPLEXES WHICH CONTAIN TWO GGAGG SEQUENCES JOINED WITH A TETRANUCLEOTIDE LINKER

Hui Liu, Atsushi Kugimiya, Tokuhiro Sakurai, Masato Katahira, and Seiichi Uesugi*

Department of Environment and Natural Sciences, Graduate School of Environment and Information Sciences, Yokohama National University, 79-7 Tokiwadai, Hodogaya-ku, Yokohama 240-8501, Japan

ABSTRACT

We have determined solution structure of r(GGAGGUUUUGGAGG) (**R14**) by NMR; the RNA 14-mer forms an intra-strand parallel quadruplex with a G-tetrad and a hexad, in which a G-tetrad core is augmented by association of two A residues. The quadruplex further forms a dimer through stacking interaction between the hexads. In order to obtain insight into the difference between RNA and DNA quadruplexes, we synthesized the corresponding DNA 14-mer, d(GGAGGTTTTGGAGG) (**D14**), and examined its properties and structure by CD, gel electrophoresis, and NMR. K^+ ions increased the thermal stability of both **R14** and **D14** structures. The binding affinity of K^+ ions to **R14** was much higher than that to **D14**. The CD and gel electrophoretic studies suggest that **D14** forms a quadruplex entirely different from that of **R14** in the presence of K^+ ions; two molecules of **D14** form a quadruplex with

*Corresponding author. Fax: +81-45-339-4265; E-mail: siuesugi@ynu.ac.jp

DOI: 10.1081/NCN-120016481 1525-7770 (Print); 1532-2335 (Online)

both antiparallel and parallel strand alignments and with diagonal loops at both ends of the stacked G-tetrads. The NMR study also gave results that are consistent with such structure: alternate glycosidic conformation, 5′G(*syn*)-G(*anti*)3′, and characteristic chemical shift data observed for many quadruplexes containing diagonal TTTT loops.

INTRODUCTION

RNA and DNA participate in many biological processes through forming various unique conformations that are highly dependent on sequences and ligands (ion, protein, drug, etc.). The guanine-rich DNA and RNA have been attracting attention for its special functions in many biological events through forming diverse quadruplex architectures that can be stabilized by monovalent cations.[1–5] The versatility of quadruplex architectures have been known by the variation in molecularity (one, two or four molecules), strand direction (parallel, antiparallel, or both), guanine glycosidic conformations (*syn* and *anti*), cations, and loop location (spanning the edge or diagonal of a G-tetrad) when loops are present. For the core of quadruplex structure, the versatility is mainly attributed to the *syn*/*anti* distribution of glycosidic conformations along each G-G step and around the G-tetrad.[6,7] In a parallel quadruplex, there is no requirement for *syn* conformation, thus, G(*anti*)-G(*anti*) for all G-G steps in each strand and G(*anti*):G(*anti*):G(*anti*):G(*anti*) arrangement for all G-tetrads are observed.[8–10] However, in a fold-back quadruplex where antiparallel strand alignment is involved, to keep the unique arrangement of guanine bases for a G-tetrad, some guanine bases must flip over. For example, in a canonical all antiparallel quadruplex that is characteristic of edgewise loops, a combination of alternating 5′G(*syn*)-G(*anti*)3′ steps and G(*syn*):G(*anti*):G(*syn*):-G(*anti*) is observed.[11–13] In a canonical parallel-antiparallel quadruplex that is characteristic of diagonal loops, a combination of alternating 5′G(*syn*)-G(*anti*)3′ steps and G(*syn*):G(*syn*):G(*anti*):G(*anti*) is observed.[14–20] In the case of d($G_3T_4G_3$), which forms a quadruplex with three G-tetrads and diagonal loops, the two asymmetric strands contain 5′G(*syn*)-G(*anti*)-G(*anti*)3′ and 5′G(*syn*)-G(*syn*)-G(*anti*)3′ segments.[21,22]

RNA quadruplexes have not been studied so intensively as DNA quadruplexes to date. However, its role in biological events are gradually realized. For example, it is reported that loss of fragile X mental retardation protein (FMRP) or dysregulation of FMRP-bound mRNA may cause the fragile X mental retardation syndrome.[16–19] FMRP are shown to bind to its own mRNA, target mRNAs and selected RNA candidates, which contain G-rich sequences and can form a quadruplex structure in vitro.[23–26] We have synthesized an RNA, r(GGAGGUUUUGGAGG) (**R14**), where two GGAGG sequences are connected by a UUUU sequence, and determined

its structure as an intra-strand parallel quadruplex forming a dimer through stacking interactions by CD and NMR.[27] Schematic diagram of its structure is shown in Fig. 1(a). Then we are interested in the structure of corresponding DNA, d(GGAGGTTTTGGAGG) (**D14**). To our knowledge, there have been only a few reports on comparison of quadruplexes formed by RNA and DNA, which contain corresponding sequences.[28–30] We examined the properties and structure of **D14** by CD, gel electrophoresis and NMR and compared with those of **R14**. We found that **D14** forms a quadruplex, which has an entirely different folding topology and shows quite different affinity for K^+ ions and thermodynamic stability.

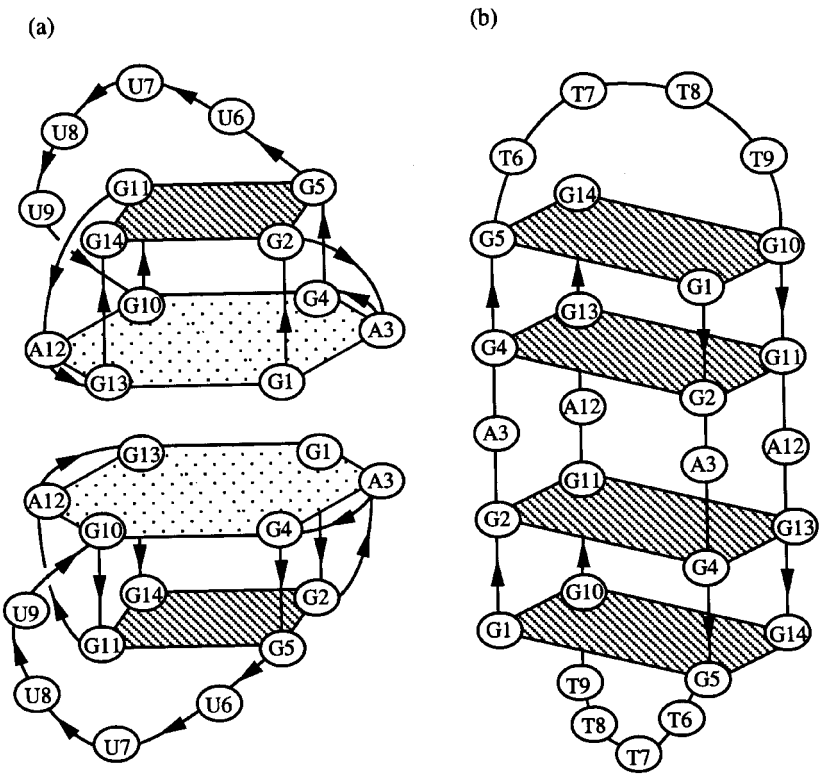

Figure 1. Schematic diagrams showing the folding topology for the structure of **R14** (a) and a possible structure of **D14** (b) in KCl solution. The rectangles and the hexagons represent the tetrads and hexads, respectively. The chain directionality is shown with arrows on the backbone tracing.

MATERIALS AND METHODS

Sample Preparation

D14 was synthesized, purified and characterized with procedures similar to those for **R14**.[27] **D14** was synthesized with a DNA/RNA synthesizer using solid-phase phosphoramidite chemistry and purified by electrophoresis on a 20% polyacrylamide gel containing 7 M urea. For CD samples, oligoneucleotides were dissolved in 300 μL buffer containing 10 mM sodium phosphate (pH 6.5) and various concentration of KCl. The concentrations of samples for CD measurement were 2 μM and 16 μM. For NMR samples, oligonucleotides were dissolved in 200 μL buffer containing 10 mM sodium phosphate (pH 6.5), 5% ^2H_2O, 0–20 mM KCl and sodium 2,2-dimethyl-2-silapentane-5-sulfonate (DSS). Samples were transferred from H_2O to ^2H_2O through lyophilization and then dissolved in 200 μL of ^2H_2O (99.96%). For NMR measurement of **R14**, the concentrations of **R14** and KCl were 1.6–2.0 mM and 0–20 mM, respectively. For NMR measurement of **D14**, the concentrations of **D14** and KCl were 0.9 mM and 0–100 mM, respectively. The CD and NMR samples were heated at 90°C for three minutes, and then cooled quickly with ice before measurement.

CD Spectroscopy

CD spectra and melting profiles were recorded with a JASCO J-720 spectropolarimeter equipped with a temperature-control unit and scanning program. A cell with 1 mm light-path length and 0.3 mL volume was used to analyze a 16 μM sample, and a cell with 1 cm light-path length and 3 mL volume was used to analyze 2 μM sample. The spectra were scanned four times from 220 nm to 320 nm at a scan speed of 10 nm/min. The CD intensities were expressed in terms of [θ] per residue. **R14** was titrated with KCl (0–500 mM) and **D14** was titrated with KCl (0–700 mM) at 5°C. To determine melting temperature, firstly the CD intensity at 265 nm, 262 nm or 295 nm was monitored increasing the temperature from 5°C to 95°C at a rate of 50°C/h, then melting temperature was obtained from the derivative of the melting curve.

NMR Spectroscopy

NMR data were collected with a Bruker DRX-600 spectrometer. Water suppression was achieved with the WATERGATE pulse[31] or with Z-axis gradients. All proton chemical shifts were measured relative to internal DSS. In 99.96% ^2H_2O, NOESY,[32] TOCSY,[33] and

^{31}P-decoupled DQF-COSY[34] spectra were recorded and analyzed as described before.[27]

RESULTS AND DISCUSSION

CD Spectral Pattern

CD spectra were measured in the presence of 0.05–500 mM KCl for **R14** (16 μM), and 30–400 mM KCl for **D14** (16 μM). Figures 2(a) and 2(c) show the effect of K^+ concentration on CD spectra of **R14** and **D14,** respectively, with some spectra omitted for clarity. In the absence of K^+, **R14** gives a positive CD band at 265 nm and a negative band at 240 nm along with a small positive band at 305 nm. The addition of K^+ ions increases [θ]s of the positive bands. This indicates that K^+ ions bind to **R14** and consequently stabilize the initial structure. Under the same experimental conditions, in the absence of K^+, **D14** shows a similar CD spectral pattern with a positive band at 262 nm and a negative band at 242 nm along with a tiny positive band at 295 nm. However, upon addition of K^+ ions to **D14**, the initial positive band at 262 nm gradually changes into the negative direction finally giving an intensive negative band. Inversion of the CD band sign also occurs for the initial negative band at 242 nm upon KCl titration finally giving a positive band at 246 nm. The initial small positive band at 295 nm gradually grows into a most intensive positive band. These CD changes suggest a conformational transition between two states since two isosbestic points are clearly observed. The change in the CD spectral pattern suggests that K^+ ion binding to **D14** causes a large conformational change and finally result in formation of an ordered structure quite different from the initial one. It is known that a parallel quadruplex gives a large positive band at around 260 nm, while a quadruplex that contains antiparallel strand orientations gives a large positive CD band at around 295 nm.[35,36] The spectral pattern of **R14** in the K^+-form is very similar to that of $d(G_4T_2G_4)$ in the presence of Na^+ ions,[35] which forms an intermolecular quadruplex containing all parallel strands. The parallel quadruplex structure of **R14** formed primarily by folding of a single molecule has been confirmed by NMR analysis.[27] On the other hand, the spectral pattern of **D14** in the K^+-form is very similar to that of $d(G_4T_4G_4)$ in the presence of Na^+ ions,[35] which forms a quadruplex containing antiparallel strands as well as parallel strands through association of two hairpins. Similar increase of a positive CD band at around 295 nm by titration with KCl has been observed for $d(G_3T_4G_3)$, which is shown by NMR and other techniques to form the antiparallel-parallel quadruplex through association of two hairpins in the presence of high concentration of K^+ or Na^+ ions.[37] These results indicate that K^+ ions can stabilize quadruplex structures for

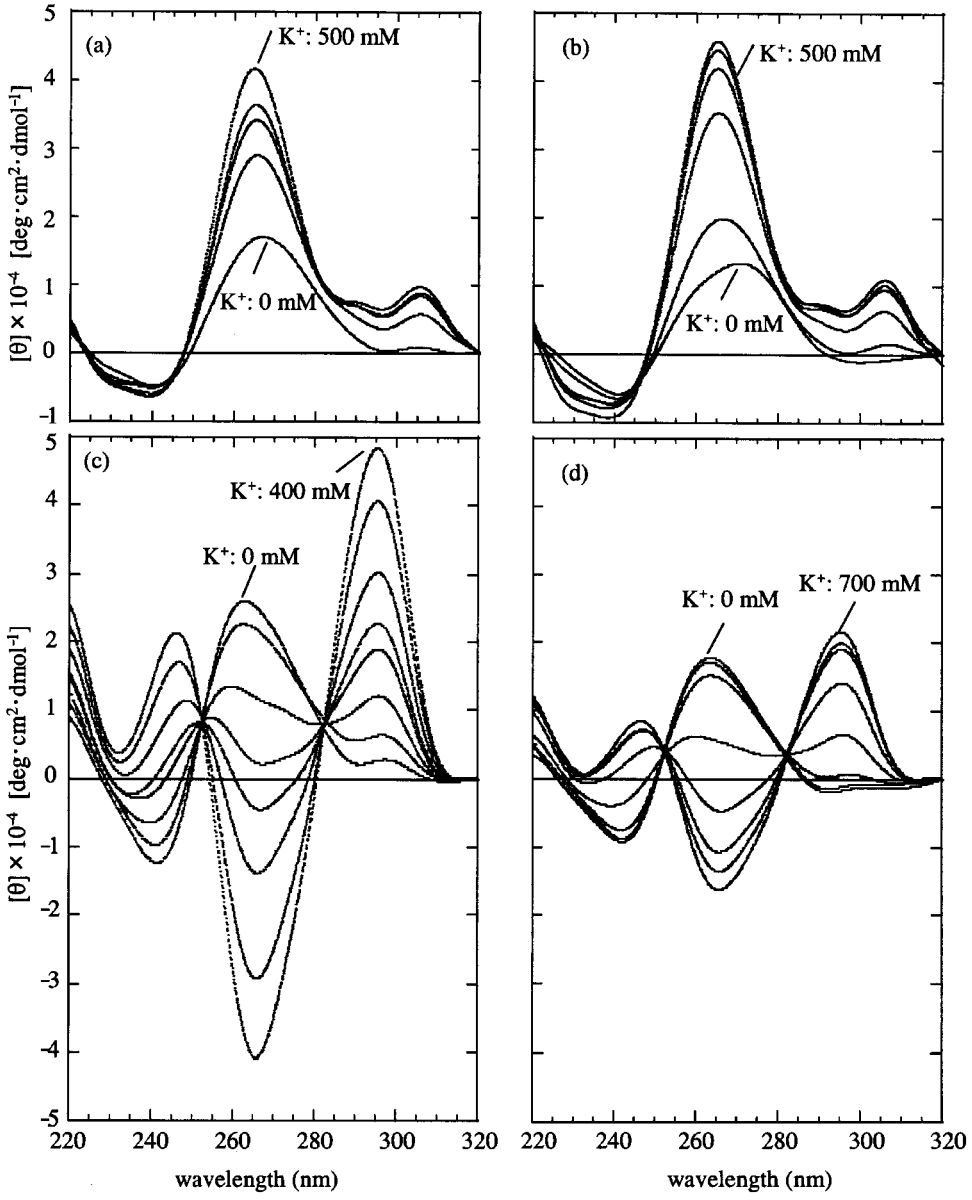

Figure 2. CD spectral changes upon KCl titration of **R14** (16 μM) (a), **R14** (2 μM) (b), **D14** (16 μM) (c) and **D14** (2 μM) (d) in 10 mM sodium phosphate (pH 6.5) at 5°C. KCl concentration: (a) 0, 0.2, 1, 50 and 500 mM; (b) 0, 1, 5, 10, 150 and 500 mM; (c) 0, 30, 40, 50, 60, 70, 100 and 400 mM; (d) 0, 40, 60, 80, 150, 300, 500 and 700 mM.

both **R14** and **D14**, and in the presence of K^+, a parallel alignment is preferred for **R14**, while an alignment containing antiparallel strands is preferred for **D14**.

Binding Affinity of K^+ to the Quadruplexes

To compare the binding affinity of K^+ ions to the quadruplexes, we plotted [θ] vs. [K^+] for **R14** and **D14** (oligomer strand concentration, 16 μM) (Fig. 3). Completely different effects of K^+ concentration on the structure of **R14** and **D14** can be clearly observed in Fig. 3. For **R14**, $[\theta]_{265}$ shows a sharp increase in the region of very low K^+ concentration, with the midpoint concentration being about 0.1 mM (Fig. 3(a) and its insert). For **D14**, the sharp decrease in the initial positive band at 262 nm and the simultaneous sharp increase in the initial tiny positive band at 295 nm occur in the region of much higher K^+ concentration (Fig. 3(b)). The midpoint concentration is estimated to be about 60 mM that is about 600-fold higher than that of **R14**, showing that the binding affinity of K^+ to **R14** is much higher than that to **D14**. Hill plot analysis of these data showed that the Hill coefficients (n) for **R14** and **D14** are 1.3 and 3.2, respectively (data not shown). These results suggest that the binding of K^+ ions to **D14** is definitely cooperative and the number of the binding K^+ ions is at least three.

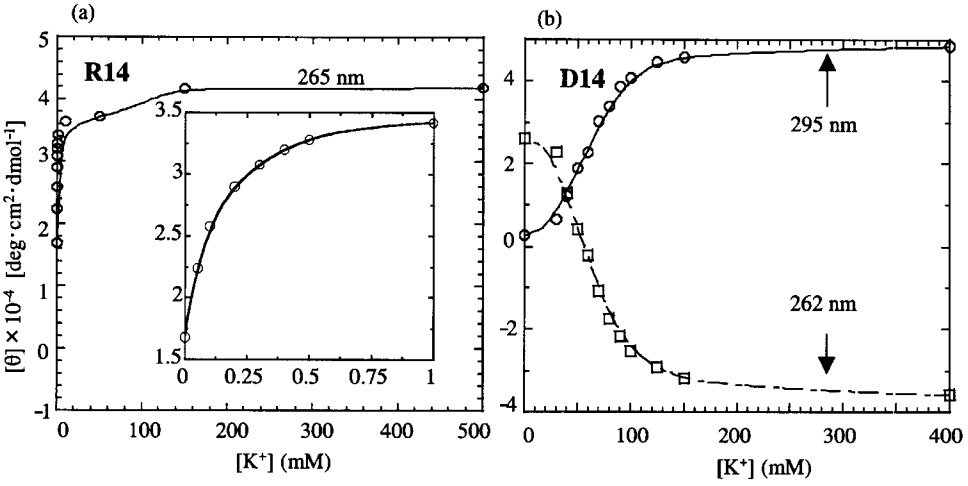

Figure 3. Effect of K^+ concentration on [θ] as monitored at 265 nm for **R14** (a), at 262 nm and 295 nm for **D14** (b). The insert in (a) shows the expanded region of 0–1 mM KCl. The samples are the same as in Fig. 2.

Effect of K^+ Concentration on Thermodynamic Stability

The melting temperatures (T_m) for the quadruplexes at different K^+ concentrations were measured by CD. The T_m vs. [K^+] plot (Fig. 4) gave curves similar to those for the [θ] vs. [K^+] plot. K^+ ions dramatically enhance thermal stability of **R14** and **D14** at different concentration ranges and by different degree. T_m of **R14** increases sharply in the much lower K^+ concentration region than that of **D14**. In the presence of 500 mM K^+, the T_m for **R14** and **D14** (oligomer concentration, 16 μM) are 86°C and 51°C, respectively. Thus the K^+-form of **R14** is much more stable than that of **D14**. The T_m vs. log[K^+] plot for these data showed that the slope for **R14** (9°C) is higher than that for **D14** (5°C). It is reported that the slope of T_m vs. log[Na^+] plot for a parallel quadruplex (14°C) is higher than that (5°C) for an antiparallel quadruplex in the system of $d(G_4T_4G_4)$.[36]

Oligonucleotide Concentration Dependency

When the oligomer concentration is reduced to 2 μM, **D14** shows much smaller CD bands in the presence of K^+ although similar CD spectral transition is observed upon titration with KCl (Fig. 2(d)). The K^+ concentration at the transition midpoint was about 240 mM, which is much higher than that (60 mM) for 16 μM **D14**. These results suggest that intermolecular association is involved in the formation of the **D14** quadruplex

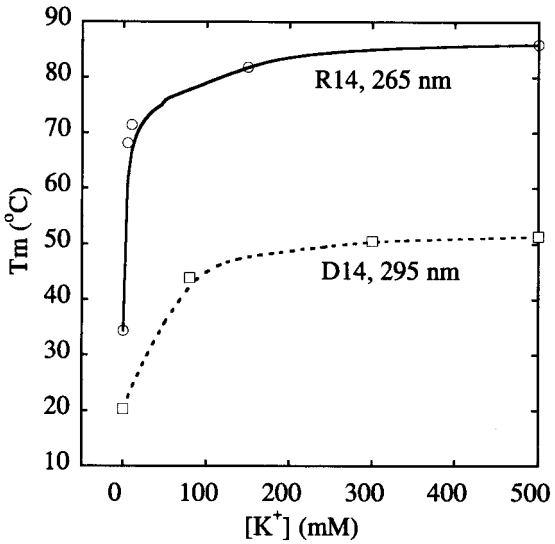

Figure 4. Effect of K^+ concentration on T_m determined by monitoring $[\theta]_{265}$ for **R14** (a), and $[\theta]_{295}$ for **D14** (b).

structure. In contrast to the case of **D14**, 2 μM **R14** shows CD spectra with almost the same pattern and intensity as those for 16 μM **R14** in the K^+ titration experiment (Fig. 2(b)). The K^+ concentration at the midpoint of the CD intensity change was about 2.2 mM which is also higher than that (0.1 mM) for 16 μM **R14**. These results indicate that the structural dependence on oligomer concentration for **R14**, which had been shown to form a dimer of intra-strand quadruplexes through intermolecular stacking,[27] is smaller than that of **D14**. The larger concentration dependency of **D14** suggests that two molecules associate through hydrogen bonding to form the quadruplex. In the case of **R14**, contribution of the stacking interactions between two quadruplex molecules may be too small to be observed clearly under the present conditions.

Gel Electrophoresis

Polyacrylamide gel electrophoresis of **R14** and **D14** on non-denaturing and denaturing gels is shown in Fig. 5. In the non-denaturing gel at 4°C, **D14** migrates much faster than $d(T_{14})$ while **R14** migrates slower than $d(T_{14})$ (Fig. 5(a)). In the denaturing gel containing 7 M urea at 40°C, **D14** migrates slightly slower than $d(T_{14})$ and **R14** also migrates slightly slower than $d(T_{14})$ (Fig. 5(b)). The electrophoretic behavior of **D14** is quite similar to that observed for a dimeric fold-back quadruplex, like $d(G_4T_4G_4)$, where $d(T_{12})$ is also used as a marker, under both non-denaturing and denaturing conditions.[35] Based on these, we propose that, in the presence of K^+, **D14** adopts a similar dimeric fold-back quadruplex, which is formed by association of

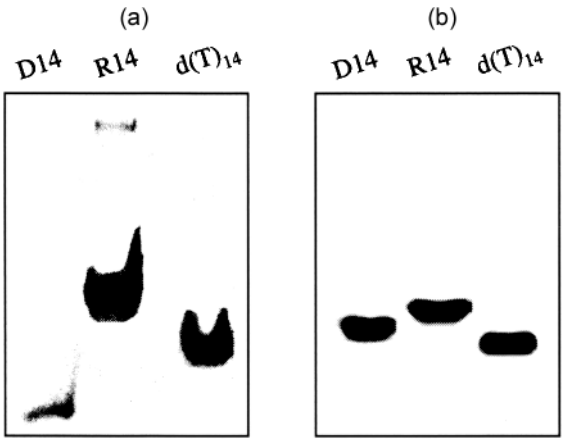

Figure 5. Electrophoretic behavior of **R14** and **D14** on 20% polyacrylamide non-denaturing gel containing 150 mM KCl at 4°C (a) and on denaturing gel containing 7 M urea at 40°C (b). Lane 1, **D14**; lane 2, **R14**; lane 3, $d(T_{14})$ marker.

two hairpins. Compared to the dimeric parallel quadruplex of **R14**, the dimeric fold-back quadruplex of **D14** is assumed to be much more compact because it shows much higher mobility in the non-denaturing gel electrophoresis. In the case of the dimeric **R14**, the UUUU loops protrude horizontally from the column of stacked G_4-tetrads and G_4A_2-hexads. This will increase the total volume of the dimeric complex resulting in lower mobility in the gel electrophoresis. Quite recently, crystal structures of similar parallel quadruplexes with TTA loops were reported for DNA oligomers containing human telomeric DNA sequences.[38]

Proton NMR Spectra

Imino proton regions of the ^{1}H NMR spectra of **R14** (2.0 mM) and **D14** (0.9 mM) in the presence of K^+ are shown in Figs. 6(a) and 6(b), respectively. **R14** and **D14** show quite different signal patterns between 11.0 ppm and 12.2 ppm, where resonances for Hoogsteen base-paired guanine imino protons are usually observed.[14,15] This result provides further evidence that

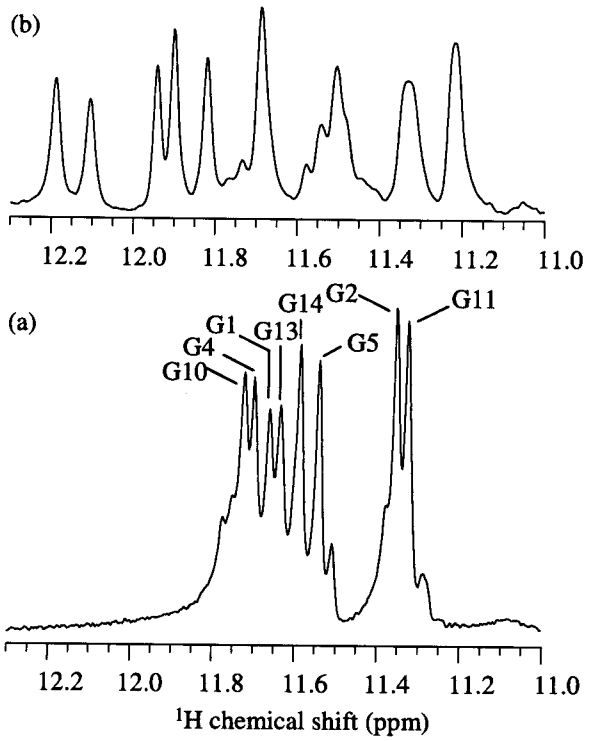

Figure 6. ^{1}H NMR spectra in the imino proton region of **R14** (2.0 mM) at 15°C (a) and **D14** (0.9 mM) at 1°C (b) in 10 mM sodium phosphate solution (pH 6.5) and KCl (20 mM for **R14** and 100 mM for **D14**). The assignments for **R14** are shown above the signals.

quadruplexes are formed in **R14** and **D14**, but the folding topologies are different. Moreover, in contrast to **R14**, the number of the observed signals in this region is larger than eight, the number of guanines in the **D14** sequence, suggesting a possibility that multiple structures coexist for **D14** in the presence of K^+. However, the global structures of the putative conformers may be very similar since the numbers of the major C–H proton signals were mostly as expected for a single major conformer although some minor signals were also observed.

NOESY Spectra

The expanded base-H1′ regions of NOESY spectra for **R14** and **D14** in ^2H_2O containing KCl are shown in Fig. 7. The sequential assignments of H1′ and H6/H8 were performed by tracing the sequential NOE connectivities between the cross-peaks for H8/H6(i)-H1′(i) and H1′(i)-H8/H6(i+1);[39] the connectivities are traced by lines in Fig. 7. It is clearly seen that the patterns of connectivities for **R14** and **D14** are quite different. The NOE connectivities for **D14** are observed for G1-G2-A3, G4-G5-T6-T7-T8-T9, G10-G11-A12,

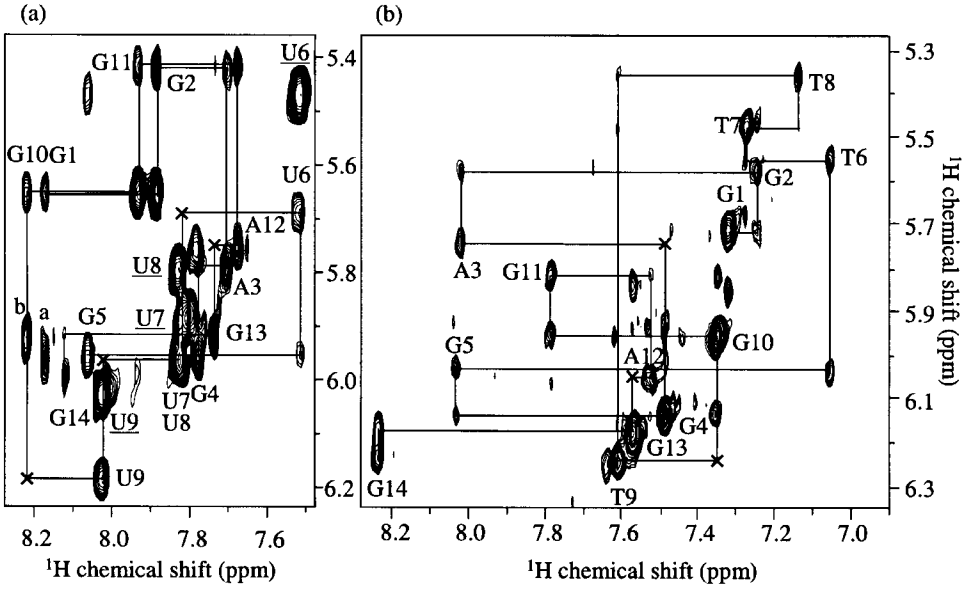

Figure 7. Expanded H6/H8-H1′ regions of NOESY spectra (230 ms mixing time) for **R14** (1.6 mM) at 32.5°C (a) and **D14** (0.9 mM) at 25°C (b) in ^2H_2O containing KCl (16 mM for **R14** and 100 mM for **D14**) and 10 mM sodium phosphate (pH 6.5). The sequential H6/H8(i)-H1′(i)-H8(i+1) connectivity is traced by lines. The intra-residue H6/H8-H1′ NOEs are labeled with the residue number and very weak or absent inter-residue H1′(i)-H8(i+1) NOEs are denoted by crosses.

and G13-G14 segments although the two GGA segments are not specifically assigned at this point. Strong intra-residue H8-H1′ NOEs for G1, G4, G10 and G13 are observed in the NOESY spectra with both 230 ms mixing time (Fig. 7) and 50 ms mixing time (data not shown), indicative of a *syn* glycosidic conformation for these four G residues.[40] The remaining residues show smaller intra-residue H8/H6-H1′ NOE cross-peaks normally observed for an *anti* conformation. Examination with molecular model building reveals that, in a 5′N(*anti*)-G(*syn*)3′ step, the distance between H1′ of N(*anti*) and H8 of G(*syn*) is much longer than those of 5′N(*anti)*-G(*anti*)3′ or 5′G(*syn*)-N(*anti*)3′ steps. Thus, it is natural that the connectivities of H1′(i)-H8/H6(i+1) are broken at all such steps, A3-G4, T9-G10 and A12-G13. Similar results have been also obtained in the case of $d(G_4T_4G_4)$[15] and $d(G_3T_4G_3)$.[21,22] These two oligomers form quadruplexes composed of two hairpins and with the same topology of folding where the G_n tracts are connected diagonally with a TTTT loop across the G-tetrad at opposite ends of stacked tetrads. The conformations of the diagonal TTTT loops for both quadruplexes and other quadruplexes[17,20] are almost identical. We found NOE corss-peaks for G1H8-T8CH_3 and G1H1′-T8CH_3, suggesting an inter-strand stacking between T8, the third T residue in the loop, and G1. Similar stacking interactions are commonly observed for corresponding residues in the quadruplexes with a diagonal TTTT loop and similar NOEs are actually observed.[15,17,22] This finding supports the assignment of the H8-H1′ cross-peaks for G1-G2-A3 and G10-G11-A12. Based on the known structure of the quadruplexes with a diagonal TTTT loop, we tentatively propose a possible model of folding topology for **D14** as shown in Fig. 1(b). At present, we have no information on the structure around the A residues. On the basis of the assignment of H8/H6 and H1′, we found that all the G-G steps take a 5′G(*syn*)-G(*anti*)3′ conformation and G-tetrads take an alignment of G(*syn*):G(*syn*):G(*anti*):G(*anti*). These structural characteristics have been observed in a group of fold-back quadruplexes with diagonal connecting loops.[14–20] Furthermore, the resonances of H6, H1′ and methyl protons of the deoxythymidine residues for **D14** have almost the same chemical shifts as those of the corresponding deoxythymidine residues of the quadruplexes. The NMR results presented here strongly support the model of the major structure for **D14** to be a quadruplex formed by two hairpin molecules with diagonal connecting loops, which is also consistent with the data of CD and gel electrophoresis studies.

Comparison of Structures and Properties of R14 and D14

The parallel quadruplex structure for **R14** is quite similar to those of d(GGAGGAN) (N = A or G)[41] and $d(GGA)_4$.[42] In the case of d(GGAGGAN), the parallel quadruplex core with G-tetrad and G,A-hexad

is formed by two molecules and the structure contains an extra A:A pair. In the case of **R14** and $d(GGA)_4$, the quadruplex core is formed intramolecularly by one molecule. It can be considered that two GGAGG segments are connected by one-residue linker, A, in $d(GGA)_4$, while **R14** has a four-residue linker. When conformational parameters for the lowest energy structures of **R14** and $d(GGA)_4$ are compared, the GGA segments of both oligomers take quite similar conformations. The G residues for each G-G step take on *anti* glycosidic conformation, S-type sugar puckering and γ mostly in the *gauche+* region, while the A residue takes on high *anti* glycosidic conformation, N-type sugar puckering and γ in the *trans* region. It is rather surprising that the GGA segments in **R14** take on the same S-S-N sugar puckering motif as that of $d(GGA)_4$ since the S-type sugar puckering is not preferable for the nucleoside residues in RNA. The unique conformation of the GGA segment may be indispensable for formation of the dimeric parallel quadruplex structure that is largely stabilized by the base-base stacking interactions. It is also surprising that the longer linker, UUUU, as well as the unfavorable sugar puckering does not seem to destabilize the parallel quadruplex structure; the T_ms are 86°C and 88°C in the presence of K^+ for **R14** and $d(GGA)_4$,[42] respectively. The presence of 2′-OH in **R14** may have special stabilizing effect, possibly through hydrogen bonding interactions. The N puckering preference of RNA can be an unfavorable factor also for **R14** to form the quadruplex containing antiparallel strand alignment since a *syn* conformation usually requires S sugar puckering.[43]

In contrast to this, **D14** forms a very different quadruplex structure, which contains antiparallel strands and *syn* glycosidic conformation, and shows much lower T_m (51°C). In the case of **D14** that does not have the stabilizing effect of 2′-OH, the longer linker, d(TTTT), may greatly destabilize the alternative intramolecular parallel quadruplex structure. On the other hand, there may be some favorable factors for the intermolecular quadruplex formation for **D14**. For instance, the d(TTTT) segment can take a stable diagonal loop conformation and the deoxyguanosine residues can easily take on a *syn* glycosidic conformation as observed in many DNA quadruplexes containing a parallel strand alignment. It is well known that the deoxynucleoside residues in DNA have little preference for sugar puckering since DNA can easily change its conformation to take B-, A- or Z-forms. The quadruplex formation for **D14** requires intermolecular association and bulged A residues. This situation may account for the observed lower stability for the **D14** quadruplex.

R14 shows much higher affinity for K^+ than **D14**. On the other hand, **D14** shows cooperative K^+ binding while **R14** does not. The reason for the higher affinity of **R14** is not well understood at present. We speculate that the UUUU loop could be responsible for the high affinity. The cooperative

K^+ binding for **D14** may be related to the intermolecular association needed for its quadruplex formation. Binding of the first K^+ ion will greatly enhance stability of G-tetrads formed by association of two molecules increasing affinity for the second K^+ ion to come in and so on. In the case of **R14**, the quadruplex core unit is formed by intra-strand folding and only one K^+ ion is needed at this stage since it contains only two G-tetrad core planes. The next stage is stacking through two hexad planes and contribution of K^+ ion for this intermolecular association may be much smaller.

CONCLUSIONS

Here we have compared structure and properties of RNA and DNA, each of which contains two GGAGG segments joined by UUUU or TTTT, respectively, as examined by CD, gel electrophoresis, and NMR. In the presence of K^+, **R14** forms an intra-strand parallel quadruplex, which consists of a G:G:G:G tetrad, a G(:A):G:G(:A):G hexad and a UUUU double-chain reversal loop, and further associates into a dimer through intermolecular hexad-hexad stacking (Fig. 1(a)), while **D14** probably forms a dimeric quadruplex with diagonal TTTT loops and with both antiparallel and parallel alignments for adjacent strands (Fig. 1(b)). The deoxyguanosine residues in the **D14** quadruplex take *syn* and *anti* conformations alternately in the G-G steps. The *syn* glycosidic conformation is usually observed in quadruplexes containing antiparallel strands. This is necessary for formation of the unique G-tetrad hydrogen-bond networks, in which the guanine bases associate in a parallel manner, when antiparallel strand alignment is involved. Since deoxynucleoside residues can adopt a *syn* glycosidic conformation, which is coupled with S sugar puckering conformation, more easily than ribonucleoside residues, **D14** may be able to form a quadruplex containing an antiparallel strand alignment by association of two diagonal hairpins in the presence of K^+. This situation is somewhat similar to that of $d(G_3T_4G_3)$ which forms a similar quadruplex stabilized by K^+ as well as Na^+.[37] K^+ ions usually stabilize parallel quadruplexes as in the case of $d(G_4T_3G_4)$ and $d(G_4T_2G_4)$, which have shorter loops.[35] In the case of $d(GGA)_4$, the DNA oligomer forms a parallel intra-strand quadruplex similar to that of **R14** in the presence of K^+, where the association of A residues through G:A pairing with one of the G-tetrad cores stabilizes the unique structure.[42] In the case of **R14**, the parallel intra-strand quadruplex structure may be stabilized by the presence of 2′-OH groups that can provide additional hydrogen-bonding capacity, and by much higher affinity for K^+ ions. Moreover, the greater difficulty in adopting a *syn* conformation for the ribonucleoside residues may make it less favorable for **R14** to form a quadruplex containing an antiparallel strand alignment.

ACKNOWLEDGMENTS

This work was supported in part by the "Research for the Future" Program (JSPS-RFTF97L00503) of the Japan Society for the Promotion of Science. M.K. was supported by Grant-in-Aid for scientific research from the Ministry of Education. Culture, Sports, Science and Technology of Japan (Nos. 10179102, 12470487 and 14035219).

REFERENCES

1. Sen, D.; Gilbert, W. Formation of Parallel Four-stranded Complexes by Guanine-rich Motifs in DNA and its Implications in Meiosis. Nature **1988**, *334* (6180), 364–366.
2. Williamson, J.R.; Raghuraman, M.K; Cech, T.R. Monovalent Cation-induced Structure of Telomeric DNA: The G-quartet Model. Cell **1989**, *59* (5), 871–880.
3. Sundquist, W.I.; Klug, A. Telomeric DNA Dimerizes by Formation of Guanine Tetrads Between Hairpin Loops. Nature **1989**, *342* (6251), 825–829.
4. Kim, J.; Cheong, C.; Moore, P.B. Tetramerization of an RNA Oligonucleotide Containing a GGGG Sequence. Nature **1991**, *351* (6324), 331–332.
5. Cheong, C.; Moore, P.B. Solution Structure of an Unusually Stable RNA Tetraplex Containing G- and U-quartet Structures. Biochemistry **1992**, *31* (36), 8406–8414.
6. Williamson, J.R. G-quartet Structures in Telomeric DNA. Annu. Rev. Biophys. Biomol. Struct. **1994**, *23*, 703–730.
7. Patel, D.J.; Bouaziz, S.; Kettani, A.; Wang, Y. Structures of Guanine-rich and Cytosine-rich Quadruplexes Formed In Vitro by Telomeric, Centromeric and Triplet Repeat Disease Sequences. In *Oxford Handbook of Nucleic Acid Structures*; Oxford University Press: Oxford, 1999; 389–453.
8. Wang, Y.; Patel, D.J. Solution Structure of a Parallel-stranded G-quadruplex Formed by d(TTGGGGT). J. Mol. Biol. **1993**, *234* (4), 1171–1183.
9. Aboud-ela, F.; Murchie, A.I.; Norman, D.G.; Lilley, D.M. Solution Structure of a Parallel-stranded Tetraplex Formed by d(TG_4T) in the Presence of Na Ions by NMR Spectroscopy. J. Mol. Biol. **1994**, *243* (3), 458–471.
10. Laughlan, G.; Murchie, A.I.; Norman, D.G.; Moore, M.H.; Moody, P.C.; Lilley, D.M.; Luisi, B. The High Resolution Crystal Structure of a Parallel-stranded Guanine Tetraplex. Science **1994**, *265* (5171), 520–524.
11. Kang, C.; Zhang, X.; Ratliff, R.; Moyzis, R.; Rich, A. Crystal Structure of Four-stranded Oxytricha Telomeric DNA. Nature **1992**, *356* (6365), 126–131.
12. Macay, R.F.; Schultze, P.; Smith, F.W.; Roe, J.A.; Feigon, J. Thrombin-binding DNA Aptamer Forms a Unimolecular Quadruplex Structure in Solution. Proc. Natl. Acad. Sci. USA **1993**, *90* (8), 3745–3749.
13. Wang, K.Y.; Krawczyk, S.H.; Bischofberger, N.; Swaminathan, S.; Bolton, P.H. The Tertiary Structure of a DNA Aptamer Which Binds to and Inhibits Thrombin Determines Activity. Biochemistry **1993**, *32* (42), 11,285–11,292.
14. Smith, F.W.; Feigon, J. Quadruplex Structure of Oxytricha Telomeric DNA Oligonucleotides. Nature **1992**, *356* (6365), 164–168.

15. Smith, F.W.; Feigon, J. Strand Orientation in the DNA Quadruplex Formed from the Oxytricha Telomere Repeat Oligonucleotide $d(G_4T_4G_4)$ in Solution. Biochemistry **1993**, *32* (33), 8682–8692.
16. Wang, Y.; Patel, D.J. Solution Structure of the Human Telomeric Repeat $d(AG_3[T_2AG_3]_3)$ G-Tetraplex. Structure **1993**, *1* (4), 263–282.
17. Wang, Y.; Patel, D.J. Solution Structure of the Oxytricha Telomeric Repeat $d[G_4(T_4G_4)_3]$ G-Tetraplex. J. Mol. Biol. **1995**, *251* (1), 76–94.
18. Smith, F.W.; Schultze, P.; Feigon, J. Solution Structures of Unimolecular Quadruplexes Formed by Oligonucleotides Containing Oxytricha Telomere Repeats. Structure **1995**, *3* (10), 997–1008.
19. Kuryavyi, V.; Kettani, A.; Wang, W.; Jones, R.; Patel, D.J. A Diamond-shaped Zipper-like DNA Architecture Containing Triads Sandwiched Between Mismatches and Tetrads. J. Mol. Biol. **2000**, *295* (3), 455–469.
20. Kuryavyi, V.; Majumdar, A.; Shallop, A.; Chernichenko, N.; Skripkin, E.; Jones, R.; Patel, D.J. A Double Chain Reversal Loop and Two Diagonal Loops Define the Architecture of a Unimolecular DNA Quadruplex Containing a Pair of Stacked G(syn)·G(syn)·G(anti)·G(anti) Tetrads Flanked by a G·(T-T) and A T·T·T Triple. J. Mol. Biol. **2001**, *310* (1), 181–194.
21. Smith, F.W.; Lau, F.W.; Feigon, J. $d(G_3T_4G_3)$ Forms an Asymmetric Diagonally Looped Dimeric Quadruplex with Guanosine 5′-*syn-syn-anti* and 5′-*syn-anti-anti* N-Glycosidic Conformations. Proc. Natl. Acad. Sci. USA **1994**, *91* (22), 10,546–10,550.
22. Keniry, M.A.; Strahan, G.D.; Owen, E.A.; Shafer, R.H. Solution Structure of the Na^+ form of the Dimeric Guanine Quadruplex $[d(G_3T_4G_3)]_2$. Eur. J. Biochem. **1995**, *233* (2), 631–643.
23. Kaytor, M.D.; Orr, H.T. RNA Targets of the Fragile X Protein. Cell **2001**, *107* (5), 555–557.
24. Schaeffer, C.; Bardoni, B.; Mandel, J.L.; Ehresmann, B.; Ehresmann, C.; Moine, H. The Fragile X Mental Retardation Protein Binds Specifically to its mRNA via a Purine Quartet Motif. EMBO J. **2001**, *20* (17), 4803–4813.
25. Brown, V.; Jin, P.; Ceman, S.; Darnell, J.C.; O'Donnell, W.T.; Tenenbaum, S.A.; Jin, X.; Feng, Y.; Wilkinson, K.D.; Keene, J.D.; Darnell, R.B.; Warren, S.T. Microarray Identification of FMRP-Associated Brain mRNAs and Altered mRNA Translational Profiles in Fragile X Syndrome. Cell **2001**, *107* (4), 477–487.
26. Darnell, J.C.; Jensen, K.B.; Jin, P.; Brown, V.; Warren, S.T.; Darnell, R.B. Fragile X Mental Retardation Protein Targets G Quartet mRNAs Important for Neuronal Function. Cell **2001**, *107* (4), 489–499.
27. Liu, H.; Matsugami, A.; Katahira, M.; Uesugi, S. A Dimeric RNA Quadruplex Architecture Composed of Two G:G(:A):G:G(:A) Hexads, G:G:G:G Tetrads and UUUU Loops. J. Mol. Biol. **2002**, *322* (5), 955–970.
28. Laughlan, G.; Murchie, A.I.H.; Norman, D.G.; Moore, M.H.; Moody, P.C.E.; Lilley, D.M.J.; Luisi, B. The High-Resolution Crystal Structure of a Parallel-stranded Guanine Tetraplex. Science **1994**, *265* (5171), 520–524.
29. Sugimoto, N.; Ohmichi, T.; Sasaki, M. The Stability of DNA and RNA G-quartets. Nucleosides Nucleotides **1996**, *15* (1–3), 559–567.

30. Deng, J.; Xiong, Y.; Sundaralingam, M. X-ray Analysis of an RNA Tetraplex $(UGGGGU)_4$ with Divalent Sr^{2+} Ions at Subatomic Resolution (0.61 Å). Proc. Natl. Acad. Sci. USA **2001**, *98* (24), 13,665–13,670.
31. Piotto, M.; Saudek, V.; Sklenar, V. Gradient-tailored Excitation for Single-quantum NMR Spectroscopy of Aqueous Solutions. J. Biomol. NMR **1992**, *2* (6), 661–665.
32. Jeener, J.; Meier, B.H.; Bachmann, P.; Ernst, R.R. Investigation of Exchange Processes by Two-dimensional NMR Spectroscopy. J. Chem. Phys. **1979**, *71*, 4546–4553.
33. Davis, D.G.; Bax, A. Assignment of Complex ^1H NMR Spectra via Two-dimensional Homonuclear Hartmann-Hahn Spectroscopy. J. Am. Chem. Soc. **1985**, *107* (9), 2820–2821.
34. Rance, M.; SøRensen, O.W.; Bodenhausen, G.; Wagner, G.; Ernst, R.R.; Wüthrich, K. Improved Spectral Resolution in COSY Proton NMR Spectra of Proteins via Double Quantum Filtering. Biochem. Biophys. Res. Commun. **1983**, *117* (2), 479–485.
35. Balagurumoorthy, P.; Brahmachari, S.K.; Mohanty, D.; Bansal, M.; Sasisekharan, V. Hairpin and Parallel Quartet Structures for Telomeric Sequences. Nucl. Acids. Res. **1992**, *20* (15), 4061–4067.
36. Lu, M.; Guo, Q.; Kallenbach, N.R. Thermodynamics of G-tetraplex Formation by Telomeric DNAS. Biochemistry **1993**, *32* (2), 598–601.
37. Scaria, P.V.; Shire, S.J.; Shafer, R.H. Quadruplex Structure of $d(G_3T_4G_3)$ Stabilized by K^+ or Na^+ is Asymmetric Hairpin Dimer. Proc. Natl. Acad. Sci. USA **1992**, *89* (21), 10,336–10,340.
38. Parkinson, G.N.; Lee, M.P.H.; Neidle, S. Crystal Structure of Parallel Quadruplexes from Human Telomeric DNA. Nature **2002**, *417* (6891), 876–880.
39. Wüthrich, K. *NMR of Proteins and Nucleic Acids*; John Wiley and Sons Inc.: New York, NY, 1986; 247–271.
40. Patel, D.J.; Kozlowski, S.A.; Nordheim, A.; Rich, A. Right-handed and Left-handed DNA: Studies of B-DNA and Z-DNA by Using Proton Nuclear Overhauser Effect and Phosphorus NMR. Proc. Natl. Acad. Sci. USA **1982**, *79* (5), 1413–1417.
41. Kettani, A.; Gorin, A.; Madjumdar, A.; Hermann, T.; Skripkin, E.; Zhao, H.; Jones, R.; Patel, D. A Dimeric DNA Interface Stabilized by Stacked A·(G·G·G·G). A Hexads and Coordinated Monovalent Cations. J. Mol. Biol. **2000**, *297* (3), 627–644.
42. Matsugami, A.; Ouhashi, K.; Kanagawa, M.; Liu, H.; Kanagawa, S.; Uesugi, S.; Katahira, M. An Intramolecular Quadruplex of $(GGA)_4$ Triplet Repeat DNA with G:G:G:G Tetrad and a G(:A):G(:A):G(:A):G Heptad, and its Dimeric Interaction. J. Mol. Biol. **2001**, *313* (2), 255–269.
43. Rao, S.T.; Sundaralingam, M. The Crystal and Molecular Structure of 3′-O-acetyladenosine. Conformational Analysis of Nucleosides and Nucleotides with *syn* Glycosidic Torsion Angle. J. Am. Chem. Soc. **1970**, *92* (16), 4963–4970.

Received July 15, 2002
Accepted August 13, 2002